

Quantum Control of Nuclear Spins*

Jonathan Hodges, Paola Cappellaro, Timothy F. Havel and David G. Cory[†]

Abstract—Nuclear Magnetic Resonance (NMR) spectroscopy has proven to be a facile means of achieving small-scale demonstrations of quantum information processing. This was in large part made possible by the sophisticated methods of quantum control that have been developed by the NMR community over a span of more than 50 years. The traditional control methods, already perhaps the most complex examples of open-loop control available, were nevertheless designed primarily to assist in identifying the physical parameters of the underlying spin system, rather than to control the system with high precision. We have therefore extended the traditional methods in a variety of ways so as to achieve precise control, by taking advantage of prior knowledge of the physical parameters as determined by traditional methods. Due to the experimental challenges of real-time control, these developments relied upon our ability to simulate the evolution of the system under the action of radio-frequency control fields with essentially arbitrary precision, subject only to the available computing power. This talk will present an overview of our work in quantum control together with some of the on-going challenges still facing us.

I. INTRODUCTION

Over the last few years quantum computing, NMR spectroscopy and classical control theory have been engaged in a fruitful exchange of ideas and methods (for examples and reviews, the reader is referred to Refs. [1], [2], [3], [4]). For the most part, this work has focused on open-loop control methods. This is due to the high dimensionality of quantum systems' state space, the nonlocal nature of "entangled" states, and the limited amount of information that can be obtained from any single measurement as a consequence of the selection rules for angular momentum state transitions. Given a quantum system that is simple enough to simulate on a classical computer, however, one has full knowledge of the state at all times and hence can use feedback to design control fields that may subsequently be applied in an open-loop fashion to the actual experimental system. This approach has been extensively utilized in our group's demonstrations of quantum computing by NMR spectroscopy [5], [6], [7]. Our purpose in this paper is to introduce the basic RF (radio-frequency) pulse sequences by which NMR spectroscopists control the nuclear spin systems with which they deal, using a matrix-oriented approach that will be familiar to control theorists, and to show how more general time-dependent RF fields which precisely effect desired operations on spin systems can be discovered using simulation and feedback.

* This work was supported by grants DAAD19-01-1-0519 & DAAD19-03-1-0125 from the U.S. Army Research Office, and by the Quantum Technologies Group of the Cambridge-MIT Institute, Ltd.

[†] All authors are affiliated with the Department of Nuclear Science and Engineering, Massachusetts Institute of Technology, Cambridge, MA 02139, USA; tfhavel@mit.edu.

II. A PRIMER ON THE THEORY OF NMR

Liquid-state NMR has proven itself a very facile experimental system with which to demonstrate the basic principles of quantum computation (*loc. cit.*). Liquid-state NMR samples are ensembles consisting of 10^{20} or more identical spin systems, each of which corresponds to the atomic nuclei within a single molecule. The fact that the molecules are in a liquid implies that the spins in different molecules interact in only a transient random fashion, so that their states, although not necessarily identical, are statistically uncorrelated; hence the term *ensemble*. For our purposes only atomic nuclei with a spin angular momentum quantum number of $1/2$ are of interest, as these constitute perfect qubits (i.e. quantum bits, which have a state space with two complex dimensions), and henceforth the term "spin" will refer only to such spins. The state space of a system containing N noninteracting spins is the tensor product of those of the individual spins, while a general state is specified by a (2^N) -dimensional complex vector $\mathbf{s} \in \mathbb{C}^N$ with $\|\mathbf{s}\| = 1$. This exponential growth in dimensionality is the origin of the power of quantum computers as compared to their classical counterparts. Although liquid-state NMR cannot, for a variety of practical reasons, be extended to systems of more than a dozen or so qubits, nuclear spins in solid-state systems remain a promising route towards large-scale quantum information processing [8], [9].

All the macroscopically observable quantities $q \in \mathbb{R}$ of an ensemble of spin systems may be expressed as real-value linear functions $q = \text{tr}(\mathbf{S}\mathbf{Q})$ of a positive-semidefinite Hermitian matrix \mathbf{S} , known as the *density matrix*. The observable quantity q itself may be identified with the Hermitian matrix \mathbf{Q} , although not every such matrix corresponds to a physically meaningful quantity. In particular, the diagonal entries of the density matrix are the probabilities of the basis states of the spins in a single molecule of the ensemble, and hence the density matrix always has unit trace. For a single molecule the spins of which are in the state \mathbf{s} , the density matrix is just $\mathbf{s}\mathbf{s}^\dagger$, while for an ensemble of M molecules it is given by the average $\mathbf{S} = \langle \mathbf{s}\mathbf{s}^\dagger \rangle = \sum_{\alpha} \mathbf{s}_{\alpha} \mathbf{s}_{\alpha}^\dagger / M$. On the other hand, for an ensemble of systems of noninteracting spins, the density matrix is just the Kronecker product of the 2×2 density matrices of the individual spins, i.e. $\mathbf{S} = \mathbf{S}_1 \otimes \cdots \otimes \mathbf{S}_N$. These two expressions are consistent since the assumption that the spins in each molecule are noninteracting implies that their states are uncorrelated across the ensemble. One of the beauties of liquid-state NMR spectroscopy is that it admits such a mathematically simple yet physically precise description.

Nuclear spins have a small magnetic dipole associated with them. In a strong magnetic field that is uniform across the ensemble, these dipoles become partially aligned with the field (although the deviations from the averages $\mathbf{s}_\alpha \mathbf{s}_\alpha^\dagger - \mathbf{S}$ remain uncorrelated). The transient interactions among the spins in different molecules, however, tend to randomize their states. According to the principles of statistical mechanics, the resulting equilibrium state has the density matrix $\mathbf{S}_{\text{eq}} = \langle \mathbf{ss}^\dagger \rangle = \exp(-\mathbf{H}/k_{\text{B}}T)/Z$, where \mathbf{H} is the Hermitian matrix that gives the energy of the spins in the magnetic field (otherwise known as the Hamiltonian), k_{B} is Boltzman's constant, T is the temperature and the partition function Z is given by $\text{tr}(\exp(-\mathbf{H}/k_{\text{B}}T))$. It is from this state that all NMR experiments must begin. Note that as $T \rightarrow \infty$, \mathbf{S}_{eq} goes to the totally random state $\mathbf{I}/2^N$, where \mathbf{I} is the identity matrix.

Quantum computers, as originally conceived, operate on a single isolated spin system, or perhaps an ensemble thereof in a pure state (meaning that all the constituent spin systems are in the same state \mathbf{s}). The first trick that was needed in order to demonstrate quantum computing by liquid-state NMR was to create an ensemble the density matrix of which had the form $\varepsilon 2^{-N} \mathbf{I} + (1 - \varepsilon) \mathbf{ss}^\dagger$, and hence defined a unique spin state (even though its constituent spin systems otherwise remained in nearly random states). Such an ensemble state is called a *pseudopure* state. The quantum control methods introduced below work identically with either pure or pseudopure states, so for our purposes we need not distinguish between them.

At this point it becomes convenient to introduce a geometric interpretation of the state space of a single spin, variously known as the Riemann, Poincare or Bloch sphere. To do this we parametrize the state (up to a physically irrelevant overall phase factor) as follows:

$$\mathbf{s} = \mathbf{s}(\vartheta, \varphi) = \begin{bmatrix} \cos(\vartheta/2) e^{i\varphi/2} \\ \sin(\vartheta/2) e^{-i\varphi/2} \end{bmatrix} \quad (1)$$

The corresponding single-spin density matrix has the form:

$$\mathbf{S} = \mathbf{ss}^\dagger = \frac{1}{2} \begin{bmatrix} 1 + \cos(\vartheta) & \sin(\vartheta) e^{i\varphi} \\ \sin(\vartheta) e^{-i\varphi} & 1 - \cos(\vartheta) \end{bmatrix} \quad (2)$$

The real and imaginary parts of the nonconstant components of this matrix are seen to correspond to the Cartesian coordinates of a unit vector given in spherical polar coordinates. These observable quantities in turn correspond to one half times the Hermitian matrices

$$\sigma_1 = \begin{bmatrix} 0 & 1 \\ 1 & 0 \end{bmatrix}, \quad \sigma_2 = \begin{bmatrix} 0 & -i \\ i & 0 \end{bmatrix}, \quad \sigma_3 = \begin{bmatrix} 1 & 0 \\ 0 & -1 \end{bmatrix}, \quad (3)$$

which are the famous Pauli matrices. For consistency, we will also use σ_0 for the 2×2 identity matrix.

The unit vector obtained in this way actually gives the direction of the magnetic dipole of the spin mentioned above. In the case of a general mixed (i.e. not pure) single-spin state, the averaging process by which we obtain the corresponding density matrix simply reduces the length of this vector, along with the net magnetic dipole of the sample. This picture is extremely useful because under a magnetic field the dipole of the spin simply precesses (rotates) about the field at a

constant rate, which corresponds to a unitary transformation $\mathbf{U}\mathbf{S}\mathbf{U}^\dagger$ of the density matrix.

We can show this by parametrizing $\text{SU}(2)$ via the Cayley-Klein parameters, i.e.

$$\mathbf{U} = \begin{bmatrix} a & -b^* \\ b & a^* \end{bmatrix}, \quad (4)$$

where $a, b \in \mathbb{C}$ with $|a|^2 + |b|^2 = 1$. Then, if $\mathbf{col} : \mathbb{R}^{2 \times 2} \rightarrow \mathbb{R}^4$ is the map which stacks the columns of a matrix on top of one another in left-to-right order, a well-known formula [10] implies

$$\mathbf{col}(\mathbf{U}\mathbf{S}\mathbf{U}^\dagger) = (\mathbf{U}^* \otimes \mathbf{U}) \mathbf{col}(\mathbf{S}), \quad (5)$$

where “ \otimes ” is the usual Kronecker product of matrices. If \mathbf{Q} is the matrix which maps the standard basis of \mathbb{R}^4 to the basis $[\mathbf{col}(\sigma_0), \mathbf{col}(\sigma_1), \mathbf{col}(\sigma_2), \mathbf{col}(\sigma_3)]/\sqrt{2}$, one readily finds that

$$\mathbf{Q}(\mathbf{U}^* \otimes \mathbf{U})\mathbf{Q}^\dagger = \begin{bmatrix} 1 & \mathbf{0}^\top \\ \mathbf{0} & \mathbf{R} \end{bmatrix}, \quad (6)$$

where \mathbf{R} is the 3×3 rotation matrix

$$\begin{bmatrix} \Re(a^2) - \Re(b^2) & \Im(a^2) - \Im(b^2) & 2\Re(a^*b) \\ -\Im(a^2) - \Im(b^2) & \Re(a^2) + \Re(b^2) & 2\Im(a^*b) \\ -2\Re(ab^*) & 2\Im(ab^*) & aa^* - bb^* \end{bmatrix}. \quad (7)$$

Similarly, one finds that $\mathbf{Q} \cdot \mathbf{col}(\mathbf{S}) = [1, \text{tr}(\sigma_1 \mathbf{S}), \text{tr}(\sigma_2 \mathbf{S}), \text{tr}(\sigma_3 \mathbf{S})]/2$ is an affine real 3-dimensional vector.

The generalization of this parametrization to larger numbers of spins is algebraically straightforward though geometrically more complicated, and allows a density matrix to be viewed as a real-valued tensor the components of which are the quantities

$$\zeta_{\alpha\beta\dots} = \text{tr}(\mathbf{S}(\sigma_\alpha \otimes \sigma_\beta \otimes \dots)) \equiv \text{tr}(\mathbf{S} \sigma_{\alpha\beta\dots}). \quad (8)$$

This is known as the *Stokes tensor* [11], and various rearrangements of it have been studied under the name of the real density matrix [12] as well as the coherence vector [13]. For $N > 1$ spins the latter is just the nonconstant (traceless) part of the vector $\mathbf{Q}^{\otimes N} \mathbf{col}(\mathbf{S})$, which likewise transforms under the real group $\text{SO}(2^N - 1)$. The usual Hermitian density matrix may be reconstructed from the Stokes tensor via the summation

$$\mathbf{S} = \sum_{\alpha,\beta,\dots=0}^{3,3,\dots} \zeta_{\alpha\beta\dots} \sigma_{\alpha\beta\dots}. \quad (9)$$

The higher-dimensional geometry underlying these algebraic facts is best understood using the completely coordinate-free approach of *geometric algebra* [14], [15]. In the following, however, we shall stick to the familiar notions of vectors and matrices.

III. NMR USING HADAMARD OPERATORS

We now consider the simple case of a rotation by the angle ϕ around the z-axis, for which the unitary matrix \mathbf{U} is diagonal with $u_{00} = \exp(-i\phi/2)$ and $u_{11} = \exp(i\phi/2)$. This

allows the unitary transformation of the density matrix to be written in a particularly simple form, namely

$$\begin{aligned} \mathbf{U}\mathbf{S}\mathbf{U}^\dagger &= \begin{bmatrix} s_{00} & e^{-i\phi} s_{10}^* \\ e^{i\phi} s_{10} & s_{11} \end{bmatrix} \\ &= \begin{bmatrix} 1 & e^{-i\phi} \\ e^{i\phi} & 1 \end{bmatrix} \odot \begin{bmatrix} s_{00} & s_{10}^* \\ s_{10} & s_{11} \end{bmatrix} \equiv \mathbf{P}_z(\phi) \odot \mathbf{S}, \end{aligned} \quad (10)$$

where “ \odot ” is the well-known *Hadamard* (or entrywise) product of matrices [10]. The Hadamard propagator $\mathbf{P}_z(\phi)$ can be expressed in terms of the Pauli matrices as $\sigma_0 + \exp(-i\sigma_3\omega t)\sigma_1$, which shows that it can be viewed as applying the rotation to the “template” σ_1 which is then imposed on the density matrix via the Hadamard product. Since NMR spectroscopists traditionally take the static magnetic field of their system as pointing along the z-axis, $\mathbf{P}_z(\omega t)$ describes how the magnetic dipole of the spins precesses about the magnetic field at ω radians / sec. In the following, we will use the Hadamard representation of diagonal unitary transformations to introduce the usual Hamiltonians of liquid-state NMR and to describe how they act on density matrices.

The most common way in which two spins interact is via ‘scalar coupling’, which has the diagonal Hamiltonian $\mathbf{H}_{zz} = (\omega/2)\sigma_{33} \equiv (\omega/2)\sigma_3 \otimes \sigma_3$. The corresponding diagonal unitary matrix $\mathbf{U}_{zz}(t) = \exp(-i\mathbf{H}_{zz}t)$ acts on the density matrix via the Hadamard propagator

$$\begin{aligned} \mathbf{P}_{zz}(\omega t) &= \begin{bmatrix} 1 & e^{-i\omega t} & e^{-i\omega t} & 1 \\ e^{i\omega t} & 1 & 1 & e^{i\omega t} \\ e^{i\omega t} & 1 & 1 & e^{i\omega t} \\ 1 & e^{-i\omega t} & e^{-i\omega t} & 1 \end{bmatrix} \\ &= \sigma_{00} + e^{-i\omega\sigma_{33}t}(\sigma_{10} + \sigma_{01}) + \sigma_{11}. \end{aligned} \quad (11)$$

If the two spins are also interacting with the applied magnetic field under the net Hamiltonian $\mathbf{H} = (\omega_{30}\sigma_{30} + \omega_{03}\sigma_{03} + \omega_{33}\sigma_{33})/2$, where we have allowed for possibly different magnetic dipoles and hence precession rates, one obtains the Hadamard propagator $\mathbf{P}_H(t) =$

$$\begin{aligned} \sigma_{00} + e^{-i\omega_{33}\sigma_{33}t} & \left(e^{-i\omega_{30}\sigma_{30}t} \sigma_{10} + e^{-i\omega_{03}\sigma_{03}t} \sigma_{01} \right) \\ & + e^{-i(\omega_{30}\sigma_{30} + \omega_{03}\sigma_{03})t} \sigma_{11} \end{aligned} \quad (12)$$

Instead of starting from the conventional Hamiltonian, exponentiating it (times it) and converting the action of the resulting unitary to a Hadamard propagator, we can define a novel kind of Hamiltonian from which the Hadamard propagator may be obtained directly via Hadamard (entrywise) exponentiation. In the simple case of a z-rotation this Hadamard Hamiltonian is just $\omega\sigma_2$, i.e. $\mathbf{P}_z(\omega t) = \exp_{\odot}(\omega\sigma_2t)$, where “ \exp_{\odot} ” denotes the Hadamard exponential. Note that we did not need to include the imaginary unit “ i ” in this expression! In a similar fashion one easily sees that $\mathbf{P}_{zz}(\omega t) = \exp_{\odot}(\omega(\sigma_{23} + \sigma_{32})t)$ and

$$\mathbf{P}_H(t) = e_{\odot}^{(\omega_{30}(\sigma_{20} + \sigma_{21}) + \omega_{03}(\sigma_{02} + \sigma_{12}) + \omega_{33}(\sigma_{23} + \sigma_{32}))t}. \quad (13)$$

The appearance of the terms σ_{12} and σ_{21} in this expression will become clear in the following paragraph.

In the usual magnetic fields used for NMR the precession frequencies of the spins are on the order of mega-Hertz, whereas the couplings among the spins are at most a few hundred Hertz – and usually much smaller. For the most part, however, it is only the differences in the precession frequencies of the spins that are of interest, and hence it is convenient to transform the dynamics into a “rotating frame”, wherein all frequencies are measured relative to that of a “carrier” signal ω_0 . Let us illustrate the above formalism by using it to describe this transformation for two spins (the generalization to any number is trivial). By definition, the rotating frame density matrix is

$$\mathbf{S}'(t) = \left(e_{\odot}^{-\omega_0\sigma_2t} \otimes e_{\odot}^{-\omega_0\sigma_2t} \right) \odot \mathbf{S}(t) \quad (14)$$

On differentiating the precession expression with respect to time and using the mixed product formula for the Hadamard and Kronecker productions (i.e. $(\mathbf{A} \odot \mathbf{B}) \otimes (\mathbf{C} \odot \mathbf{D}) = (\mathbf{A} \otimes \mathbf{C}) \odot (\mathbf{B} \otimes \mathbf{D})$), we obtain

$$\dot{\mathbf{S}}'(t) = \left(((\omega_0\sigma_2) \otimes \mathbf{J}) + (\mathbf{J} \otimes (\omega_0\sigma_2)) \right) \odot \mathbf{S}'(t), \quad (15)$$

where $\mathbf{J} = \sigma_0 + \sigma_1$ is a 2×2 matrix of all ones. It follows that

$$\begin{aligned} \dot{\mathbf{S}}'(t) &= \left(\frac{d}{dt} \left(e_{\odot}^{-\omega_0\sigma_2t} \otimes e_{\odot}^{-\omega_0\sigma_2t} \right) \odot \mathbf{P}_H(t) + \right. \\ & \left. \left(e_{\odot}^{-\omega_0\sigma_2t} \otimes e_{\odot}^{-\omega_0\sigma_2t} \right) \odot \left(\frac{d}{dt} \mathbf{P}_H(t) \right) \right) \odot \mathbf{S}(0) \\ &= ((\omega_{30} - \omega_0)(\sigma_{20} + \sigma_{21}) + \\ & \quad (\omega_{03} - \omega_0)(\sigma_{02} + \sigma_{12}) + \\ & \quad \omega_{33}(\sigma_{23} + \sigma_{32})) \odot \mathbf{S}'(t), \end{aligned} \quad (16)$$

i.e. the precession frequencies are now relative to ω_0 as claimed. Henceforth all our density matrices \mathbf{S} and precession frequencies ω_{30} etc. will be referenced to a rotating frame, unless otherwise specified.

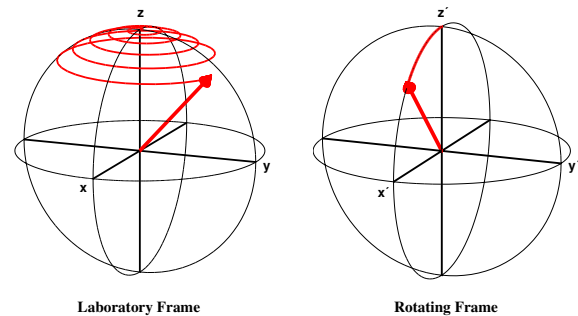


Fig. 1. Rotation of the Bloch vector of a spin about the y-axis in the laboratory frame (right) and in the rotating frame (left).

The final issue which it is convenient to tackle with Hadamard products is decoherence, which is the diffusive effect of many small random rotations about the z-axis due to interaction with other molecules in the ensemble. Since these rotations act independently on all members of the ensemble, all the off-diagonal components of the density matrix decay

gradually to zero. For a single spin with a zero-mean random rotation rate ω , we can describe this by the corresponding average Hadamard propagator,

$$\begin{aligned} \langle \mathbf{P}_z(\omega t) \rangle &= \begin{bmatrix} 1 & \langle \exp(-i\omega t) \rangle \\ \langle \exp(i\omega t) \rangle & 1 \end{bmatrix} \\ &= \sigma_0 + \langle \cos(\omega t) \rangle \sigma_1 \approx \sigma_0 + e^{-\langle \omega^2 \rangle t} \sigma_1 \\ &= \exp_{\odot}(-\langle \omega^2 \rangle \sigma_1 t) \end{aligned} \quad (17)$$

For two spins with statistically independent rotation rates ω_{30} and ω_{03} , we obtain

$$\begin{aligned} \langle \mathbf{P}_z(\omega_{30} t) \rangle \otimes \langle \mathbf{P}_z(\omega_{03} t) \rangle &\approx \sigma_{00} + \\ e^{-\langle \omega_{30}^2 \rangle t} \sigma_{10} + e^{-\langle \omega_{03}^2 \rangle t} \sigma_{01} + e^{-((\omega_{30}^2) + (\omega_{03}^2)) t} \sigma_{11} & \quad (18) \\ = e_{\odot}^{-((\omega_{30}^2) \sigma_{10} + (\omega_{03}^2) \sigma_{01} + ((\omega_{30}^2) + (\omega_{03}^2)) \sigma_{11}) t} & \end{aligned}$$

The extension of this result to any number of spins is straightforward.

IV. REFOCUSING UNWANTED EVOLUTIONS

The above Hadamard formalism applies only to interactions that are diagonal in the usual representation by tensor products of Pauli matrices. Rotations about axes other than the z-axis can, of course, be expressed by rotation $\mathbf{R}(\theta)$ about some axis in the xy-plane, followed by a z-rotation by ϕ and then the inverse rotation $\mathbf{R}(-\theta) = \mathbf{R}^\dagger(\theta)$, i.e.

$$\mathbf{R}^\dagger(\theta) (\mathbf{P}_z(\phi) \odot (\mathbf{R}(\theta) \mathbf{S} \mathbf{R}^\dagger(\theta))) \mathbf{R}(\theta). \quad (19)$$

Unfortunately, sequences of general rotations rapidly become unwieldy in this notation. In the special case of a rotation by π about the e.g. x-axis, however, we have $\mathbf{R}(\pi) = -i\sigma_1$, and hence

$$\begin{aligned} &\sigma_1 (\mathbf{P}_z(\phi) \odot (\sigma_1 \mathbf{S} \sigma_1)) \sigma_1 \\ &= \sigma_1 \left(\begin{bmatrix} 1 & e^{-i\phi} \\ e^{i\phi} & 1 \end{bmatrix} \odot \begin{bmatrix} s_{11} & s_{10} \\ s_{10}^* & s_{00} \end{bmatrix} \right) \sigma_1 \\ &= \begin{bmatrix} 1 & e^{i\phi} \\ e^{-i\phi} & 1 \end{bmatrix} \odot \begin{bmatrix} s_{00} & s_{10}^* \\ s_{10} & s_{11} \end{bmatrix} = \mathbf{P}_z(-\phi). \end{aligned} \quad (20)$$

In other words, sandwiching a z-rotation between a pair of π -rotations (about any axis in the xy-plane) simply reverses the sense of the z-rotation.

In the case of continuous precession about the z-axis, therefore, the application of a pair of π -rotations separated by a period τ results in no *net* precession a period τ after the second. A little thought will actually show that the π -rotations can be placed anywhere in an interval of length 2τ , providing they are τ apart. The rotations themselves are effected by applying an RF (radio-frequency) field that is synchronous with the precession rate, and thus in the rotating frame looks like a static magnetic field in the xy-plane (cf. Fig. 1). These fields normally effect a rotation by π in a period short compared to τ , and hence are called π -pulses. The pair of π -pulses is said to *refocus* the precession, in effect turning off the interaction of the spins with the static magnetic field. The ability to refocus unwanted interactions is of the utmost importance for quantum information processing by NMR, since one usually wants a

sequence of simple well-defined evolutions to occur and not many different, and usually undesired, interactions at once. In the following we will consider a few more interesting examples.

Given a pair of spins coupled by a σ_{33} interaction, the application of a pair of π -pulses to just one of the spins refocuses both the precession of that spin as well as the scalar coupling between them. This may be shown in a fashion similar to that seen above for the precession alone. In reality, however, the scalar coupling between the spins has a (conventional) Hamiltonian proportional to $\sigma_{11} + \sigma_{22} + \sigma_{33}$, which is more difficult to refocus. It can nevertheless be done by a sequence of four equally spaced π -pulses, the first and third of which are $\pi/2$ out-of-phase with respect to the second and fourth (e.g. about the x and y-axes, respectively). Of greater interest here is the fact that whenever the difference $|\omega_{30} - \omega_{03}| \gg \omega_{33}$ one can neglect the $\sigma_{11} + \sigma_{22}$ term. This is because the $\sigma_{30} - \sigma_{03}$ part of the Hamiltonian rapidly refocusses the $\sigma_{11} + \sigma_{22}$ part, as will now be shown.

We begin by writing the full (or strong) two-spin NMR Hamiltonian in the form

$$\begin{aligned} \mathbf{H} &= \underbrace{\frac{\omega_-}{2} (\sigma_{30} - \sigma_{03})}_{\mathbf{A}} + \underbrace{\frac{\Omega}{2} (\sigma_{11} + \sigma_{22})}_{\mathbf{B}} \\ &+ \underbrace{\frac{\omega_+}{2} (\sigma_{30} + \sigma_{03}) + \frac{\Omega}{2} \sigma_{33}}_{\mathbf{C}}, \end{aligned} \quad (21)$$

where $\omega_- = (\omega_{30} - \omega_{03})/2$, $\omega_+ = (\omega_{30} + \omega_{03})/2$, and Ω is the scalar coupling. Note that while \mathbf{C} commutes with both \mathbf{A} and \mathbf{B} , the propagator $\exp(i\pi/\omega_- \mathbf{A})$ anti-commutes with \mathbf{B} . Thus when $\omega_- t = 2\pi$, we obtain $\exp(-it\mathbf{H})$

$$\begin{aligned} &\approx \left(e^{-it\mathbf{A}/4} e^{-it\mathbf{B}/2} e^{-it\mathbf{A}/2} e^{-it\mathbf{B}/2} e^{-it\mathbf{A}/4} \right) e^{-it\mathbf{C}} \\ &= \left(e^{-3it\mathbf{A}/4} e^{it\mathbf{B}/2} e^{-it\mathbf{B}/2} e^{-it\mathbf{A}/4} \right) e^{-it\mathbf{C}} = e^{-it(\mathbf{A}+\mathbf{C})}. \end{aligned} \quad (22)$$

This approximation is accurate to $O((\Omega/\omega_-)^2)$.

Another good refocusing trick which is amenable to a similar analysis is the use of train of π -pulses to refocus the precession of the two spins, thereby effectively setting $\omega_- = 0$ and reintroducing the $\sigma_{11} + \sigma_{22}$ terms into the Hamiltonian. Essentially the same procedure can also be used to correct for a dispersion in the rates at which the spins in different molecules of the ensemble rotate, due to spatial inhomogeneity in the RF fields across the sample; this illustrated in Fig. 2 below. In the continuous version of this trick, known as *spin locking*, the spins are first rotated to the x-axis of the rotating frame, and a strong RF field applied with a frequency ω that is nearly synchronous with the spins' precession. As long as the amplitude of this RF field is large compared to ω_- , every time the spins start to get a bit out of sync with the field they quickly rotate by π about the field and hence precess back to where they came.

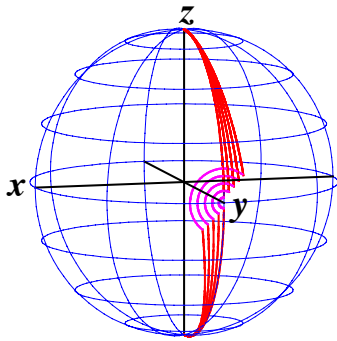


Fig. 2. Each line on the Bloch sphere represents a rotation at slightly different rates about an axis in the xy -plane. A composite π -pulse breaks the overall rotation down into two $\pi/2$ rotations, separated by another rotation by π about an axis perpendicular to the axis of the $\pi/2$ rotations. Even though the intervening rotation also does not achieve exactly the intended rotation by π , may be seen that the composite pulse refocusses a range of rotation rates due to inhomogeneity of the RF fields across the ensemble.

V. FINDING COMPLEX CONTROL FIELDS BY SIMULATION AND OPTIMIZATION

While all these refocussing tricks are useful in understanding NMR techniques, they are directly applicable only to the simplest experiments. When many different interactions must be simultaneously refocused in order to implement a single desired net unitary transformation, a (classical) computer must be used to find a sequence of fields that can achieve this. One can be sure that a solution exists only if the strength of the RF fields one can apply are strong (i.e. rotate the spins rapidly) compared to their range of precession frequencies and the strongest interaction among them. Such *strongly modulating* pulses allow one to essentially dominate the internal dynamics of the spin system and hence obtain universal control over the dynamics.

One caveat to be mentioned in this regard is the fact that when a molecule contains nuclear spins from different isotopes (e.g. ^1H and ^{13}C), their precession frequencies will span a range of mega-Hertz, far beyond the strongest RF fields. Fortunately, in this extreme case the RF fields needed to address one kind of nucleus are generally so far off-resonance from the other spins that they are totally unaffected by it. This makes it possible to use a completely independent RF channel for each kind of nucleus, and so put each in an independent rotating frame. The large frequency differences among spins of different nuclei also guarantees that the coupling between them is weak, i.e. described by Hamiltonians of the form σ_{33} , with no possibility of inadvertently reintroducing the transverse terms $\sigma_{11} + \sigma_{22}$ among them.

The equation of motion for the density matrix \mathbf{S} under the action of the Hamiltonian \mathbf{H} is expressed as

$$\dot{\mathbf{S}}(t) \equiv d\mathbf{S}/dt = i[\mathbf{S}(t), \mathbf{H}(t)]. \quad (23)$$

The formal solution at a time t_1 given the initial condition $\mathbf{S}(t_0)$ is $\mathbf{S}(t_1) = \mathbf{U}(t_0, t_1)\mathbf{S}(t_0)\mathbf{U}^\dagger(t_0, t_1)$, where \mathbf{U} is the unitary matrix:

$$\begin{aligned} \mathbf{U}(t_0, t_1) &= \hat{\mathbf{T}} \exp\left(-i \int_{t_0}^{t_1} dt' \mathbf{H}(t')\right) \\ &\equiv \lim_{n \rightarrow \infty} e^{-i\Delta_n t} \mathbf{H}(t_0 + \Delta_n t) e^{-i\Delta_n t} \mathbf{H}(t_0 + 2\Delta_n t) \dots e^{-i\Delta_n t} \mathbf{H}(t_0 + t_1) \end{aligned} \quad (24)$$

Here $\hat{\mathbf{T}}$ is the Dyson time-ordering operator, which in combination with the integral in the exponent symbolizes the limit of the time-ordered product indicated on the second line (wherein $\Delta_n t \equiv (t_1 - t_0)/n$).

Unfortunately this formal solution is both difficult and time-consuming to evaluate in general, and we have therefore greatly simplified the problem by assuming that our control fields have a phase, amplitude and frequency which is piecewise constant in time. By transformation into a rotating frame wherein the Hamiltonian \mathbf{H}'_k in each such interval is time-independent, we can reduce the above infinite product to a finite (and usually quite short) product of simple matrix exponentials, of the form

$$\mathbf{U}(t_{k-1}, t_k) = \exp(-i(t_k - t_{k-1})\mathbf{H}'_k). \quad (25)$$

($k = 1, \dots, N$). The Hamiltonians describing the interaction between our control fields and the spins all have the form

$$\begin{aligned} \mathbf{h}_k^\alpha(t) &= \Omega_k^\alpha e^{-i(\omega_k^\alpha t + \varphi_k^\alpha)} \sigma_3^\alpha / 2 \sigma_1^\alpha e^{-i(\omega_k^\alpha t + \varphi_k^\alpha)} \sigma_3^\alpha / 2 \\ &= \Omega_k^\alpha e_{\odot}^{-i(\omega_k^\alpha t + \varphi_k^\alpha) \Sigma_3^\alpha} \odot \sigma_1^\alpha, \end{aligned} \quad (26)$$

where $\alpha \subseteq \{1, \dots, S\}$ is the set of indices labeling all $|\alpha\rangle$ spins of a given isotope, ω_k^α is the frequency of the control field close enough to resonance with that isotope to interact significantly with the corresponding spins, Ω_k^α is the field's amplitude, φ_k^α is its initial phase, $\sigma_1^\alpha \equiv \sigma_1^{\alpha_1} + \dots + \sigma_1^{\alpha_{|\alpha|}}$ and similarly for σ_3^α , and finally $\Sigma_3^\alpha \equiv \mathbf{diag}(\sigma_3^\alpha) \mathbf{diag}^\dagger(\sigma_3^\alpha)$ (where $\mathbf{diag}(\sigma_3^\alpha)$ is the column vector formed from the diagonal entries of σ_3^α).

The time-dependence of the control fields may be removed by applying the inverse (up to a phase factor) of the Hadamard operator for each channel, namely $\exp_{\odot}(i\omega_k^\alpha t \Sigma_3^\alpha)$, to the untransformed Hamiltonian, which yields

$$\mathbf{H}'_k = e_{\odot}^{i t \sum_{\alpha} \omega_k^\alpha \Sigma_3^\alpha} \odot \mathbf{H}_k = \mathbf{H}_{\text{int}} + \sum_{\alpha} e_{\odot}^{i t \omega_k^\alpha \Sigma_3^\alpha} \odot \mathbf{h}_k^\alpha(t). \quad (27)$$

Here, \mathbf{H}_{int} is the (time-independent) internal Hamiltonian of the spin system when no control fields are present, which commutes with the σ_3^α operators and hence is invariant under the frame transformation (both in the strong as well as the weak coupling regime). Although the exponential growth in the size of the Hamiltonians with the number of spins prevents us from calling this approach "efficient", it does allow us to accurately simulate the dynamics of up to about a dozen spins on a modern personal computer. Further details regarding how the spin system is modeled may be found in Ref. [7].

We have extensively explored such a numerical approach to designing fast, high-fidelity pulses which rotate various combinations of spins and axes in the xy -plane, usually by π or $\pi/2$ [16], [17]. Such single qubit gates are a basic and essential operation needed for NMR quantum computation,

and in combination with periods of free evolution under \mathbf{H}_{int} allow any unitary operation on the spins to be implemented by fairly standard pulse sequence design methods from NMR (see e.g. Ref. [18]). The basic search procedure is outlined in Fig. 3 below. We start by choosing control fields with constant amplitude, frequency and phase which approximately implement the desired rotations on the intended subset of spins over a single time interval, but which would generally have non-negligible effects on the unintended spins as well. This interval is broken into a small number (3 or 4) of time intervals $\{\tau_k\}_{k=1,\dots,N}$ in each of which the amplitude, frequency and phase of the control fields are held constant, a simplex of other parameter values chosen at random in its vicinity, and these parameters varied according to the well-known simplex algorithm (as implemented in the `MatLab`TM programming system), until the simulated unitary matrix is essentially identical to the desired unitary \mathbf{U}_o – or it becomes clear that the search is not converging. In the latter case one tries again with different initial control fields and/or simplex, or if need be creates additional time intervals and hence further parameters to vary. The comparison function passed to the simplex minimization routine is

$$f\left(\left\{\Omega_k^\alpha, \omega_k^\alpha, \phi_k^\alpha, \tau_k\right\}_{k=1,\dots,N}^{\alpha \in \{1,\dots,S\}}\right) \equiv 1 - 2^{-N} \left| \text{tr} \left(\mathbf{U}_o^\dagger \mathbf{U} \left(\left\{\Omega_k^\alpha, \omega_k^\alpha, \phi_k^\alpha, \tau_k\right\}_{k=1,\dots,N}^{\alpha \in \{1,\dots,S\}} \right) \right) \right|^2, \quad (28)$$

where $\mathbf{U}(\dots)$ is the unitary determined by simulation, and $|\dots|$ denotes the complex absolute value. Although not included here for the sake of brevity, in practice the comparison function will also include further terms in order to penalize solutions which require more power than the NMR spectrometer can provide, intervals too short to be implemented given the spectrometer's transients, and other such physical constraints.

The simplex method is, of course, not guaranteed to find the global minimum, but experience indicates that acceptably good, albeit local, minima constitute a nontrivial fraction of the total, at least once the number of intervals used, and hence the number of parameters to play with, gets large enough. In a related approach [19], many equal-length time intervals are used, and hence many more parameters need to be varied. This precludes use of the simplex method, and hence a quadratically convergent optimization method such

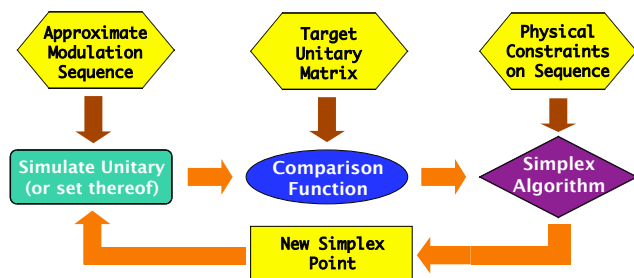


Fig. 3. The search procedure used to find strongly modulating radio-frequency pulses which precisely implement a desired unitary transformation for a given kind of molecule.

as conjugate gradients is used instead. This in turn requires the gradients of f , which are computed using techniques similar to those described in Ref. [20]. In our experience both approaches yield valid, experimentally practical results, but the simplex-based approach generally finds solutions with far fewer time intervals, and which are therefore somewhat easier to understand (see example below). In addition, the simulation of the target unitary matrix is the most time-consuming part of any search procedure, and the time required is proportional to the number of matrix exponentials and hence the number of time intervals.

Strongly modulating pulse example

As an illustrative example, we use the four spin-1/2 ^{13}C nuclei in Crotonic Acid, whose chemical structure and Hamiltonian's parameters are shown in Fig. 4. It may be

	1	2	3	4
1	11617.9	72.4	-1.4	7.0
2		52.0	7850.4	69.7
3			1323	27.5
4				1660

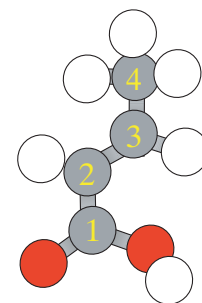


Fig. 4. The chemical structure of Crotonic Acid is shown on the right, with the ^{13}C nuclei numbered as in the table on the left. The resonance frequencies of the carbons relative to carbon 4 are shown along the diagonal in Hz, while the couplings among them are shown above the diagonal in Hz, and the ratios of the frequency differences to the couplings are shown below the diagonal.

seen that the resonance frequencies of spins 1 and 3 differ by less than 2000 Hz, making it impossible to find a simple irradiation scheme which rotates spin 1 by $\pi/2$ in less than a millisecond without affecting spin 3. Nevertheless, our pulse-finding procedure was able to discover a sequence of *HOW MANY???* intervals which rotates spin 1 by $\pi/2$ with no *net* effect upon the other spins, and in a total of only *HOW MANY???* microseconds. As may be seen in Fig. 5, this is not because the other spins were not affected, but rather because the control sequence returns them to their starting positions at the end of the last interval. We note also that, although the hydrogens were not included in the simulations by which this control sequence was found, the rather chaotic motion of the spins under the strong fields used tended to decouple them from their attached carbons, even though these couplings are of order 150 Hz.

VI. CLOSING REMARKS

It should be noted that, like all exact simulations of many-body quantum systems on classical computers, the above procedure for finding time-dependent control fields that implement a desired unitary operation is highly exponential in the number of spins. Thus these control methods are certainly not scalable to systems with more than about a

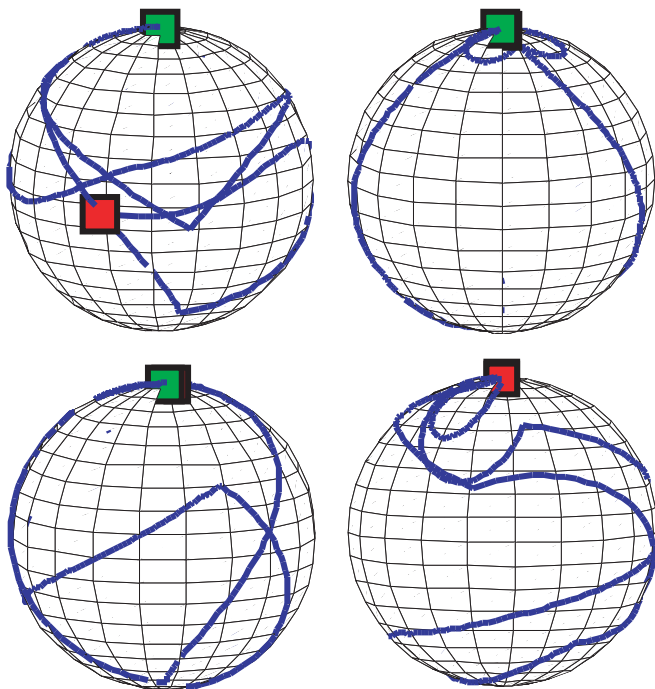


Fig. 5. Spin trajectories for a control sequence which rotates only the first carbon spin of Crotonic Acid by $\pi/2$ (cf. Fig. 4). The green squares on each Bloch sphere indicate the initial states (along \hat{z} for all spins) while the red squares indicate the final state. Observe that all spins except the first return to their initial positions, as desired. Discontinuities of the trajectory on the surface are due to abrupt switching between consecutive intervals of constant amplitude, frequency and phase.

dozen qubits in them – which is about as large as liquid-state NMR can hope to handle experimentally. Just as happened over the course of the development of today’s computers, it may be possible to use small quantum computers to bootstrap up to larger and larger spin systems, in effect substituting experiments for computation. Otherwise, any scalable pulse design method will have to make simplifying approximations, the accuracy of which will depend on the details of the physical system to which they are applied.

Chief among these will doubtless be the ability actually turn off, and not merely refocus, the evolution of the qubits over large portions of the spin system. This is implicitly assumed in nearly all theoretical studies of quantum information processing, but may be rather difficult to obtain in practice. For example, the dipole-dipole interaction among the spins in solid-state NMR falls off as the inverse cube of the distance between them, which although faster than electrostatic monopole interactions still allows for a relatively dense network of interactions among them. It has recently been shown that in certain simple situations one can effectively decouple the weak interactions among spins while selectively leaving the stronger ones active, thereby simplifying the interaction network [21], [22]. Extending this capability to the dipole-dipole interactions among all but the nearest neighbor spins in an e.g. cubic lattice remains an important open problem.

REFERENCES

- [1] R. Laflamme, E. Knill, D. G. Cory, E. M. Fortunato, T. F. Havel, C. Miquel, R. Martinez, C. Negrevergne, G. Ortiz, M. A. Pravia, Y. Shart, S. Sinha, R. Somma, and L. Viola, “Introduction to NMR quantum information processing,” *Los Alamos Science*, vol. 27, pp. 2–37, 2002.
- [2] L. M. K. Vandersypen and I. L. Chuang, “NMR techniques for quantum control and computation,” *Rev. Mod. Phys.*, vol. 76, 2004.
- [3] C. Altafini, “Coherent control of open quantum system dynamics,” *Phys. Rev. A*, vol. 70, p. 062321, 2004.
- [4] H. Mabuchi and N. Khaneja, “Principles and applications of control in quantum systems,” *Intl. J. Robust Nonlinear Control*, vol. 15, pp. 647–667, 2005.
- [5] T. F. Havel, D. G. Cory, S. Lloyd, N. B. E. M. Fortunato, M. A. Pravia, G. Teklemariam, Y. S. Weinstein, A. Bhattacharyya, and J. Hou, “Quantum information processing by nuclear magnetic resonance spectroscopy,” *Am. J. Phys.*, vol. 70, pp. 345–362, 2002.
- [6] S. Sinha, J. Emerson, N. Boulant, E. M. Fortunato, T. F. Havel, and D. G. Cory, “Experimental simulation of spin squeezing by nuclear magnetic resonance,” *Quantum Information Processing*, vol. 2, pp. 433–448, 2003.
- [7] Y. S. Weinstein, T. F. Havel, J. Emerson, N. Boulant, M. Saraceno, S. Lloyd, and D. G. Cory, “Quantum process tomography of the quantum Fourier transform,” *J. Chem. Phys.*, vol. 121, pp. 6117–6133, 2004.
- [8] D. G. Cory, R. Laflamme, E. Knill, L. Viola, T. F. Havel, N. Boulant, G. Boutis, E. Fortunato, S. Lloyd, R. Martinez, C. Negrevergne, M. Pravia, Y. Sharf, G. Teklemariam, Y. S. Weinstein, and Z. H. Zurek, “NMR based quantum information processing,” *Prog. Phys.*, vol. 48, pp. 875–907, 2000.
- [9] J. Baugh, O. Moussa, C. A. Ryan, R. Laflamme, C. Ramanathan, T. F. Havel, and D. G. Cory, “Solid-state NMR three-qubit homonuclear system for quantum-information processing: Control and characterization,” *Phys. Rev. A*, vol. 73, p. 022305, 2006.
- [10] H. Lütkepohl, *Handbook of Matrices*. New York, NY: John Wiley & Sons, 1996.
- [11] C. Altafini, “Representing multiqubit unitary evolutions via Stokes tensors,” *Phys. Rev. A*, vol. 70, p. 032331, 2004.
- [12] T. F. Havel, “The real density matrix,” *Quantum Inform. Processing*, vol. 1, pp. 511–538, 2002.
- [13] M. S. Byrd and N. Khaneja, “Characterization of the positivity of the density matrix in terms of the coherence vector representation,” *Phys. Rev. A*, vol. 68, p. 062322, 2003.
- [14] T. F. Havel and C. Doran, “Geometric algebra in quantum information processing,” in *Quantum Information and Computation*, ser. Contemporary Mathematics, S. J. Lomonaco, Jr. and H. E. Brandt, Eds., vol. 305. Am. Math. Soc., Providence, RI, 2002, pp. 81–100, (see also LANL preprint quant-ph/0004031).
- [15] C. Doran and A. Lasenby, *Geometric Algebra for Physicists*. Cambridge, U.K.: Cambridge Univ. Press, 2003.
- [16] E. M. Fortunato, M. A. Pravia, N. Boulant, G. Teklemariam, T. F. Havel, and D. G. Cory, “Design of strongly modulating pulses to implement precise effective hamiltonians for quantum information processing,” *J. Chem. Phys.*, vol. 116, pp. 7599–7606, 2002.
- [17] M. A. Pravia, N. Boulant, J. Emerson, A. Farid, E. M. Fortunato, T. F. Havel, R. Martinez, and D. G. Cory, “Robust control of quantum information,” *J. Chem. Phys.*, vol. 119, pp. 9993–10001, 2003.
- [18] M. Mehring and V. A. Weberruss, *Object-Oriented Magnetic Resonance*. Elsevier Science and Technology Books, 2001.
- [19] T. E. Skinner, K. Kobzar, B. Luy, M. R. Bendall, W. Bermel, N. Khaneja, and S. J. Glaser, “Optimal control design of constant amplitude phase-modulated pulses: Application to calibration-free broadband excitation,” *J. Magn. Reson.*, 2006, in press.
- [20] I. Najfeld and T. F. Havel, “Derivatives of the matrix exponential and their computation,” *Adv. Appl. Math.*, vol. 16, pp. 321–375, 1995.
- [21] C. Ramanathan, S. Sinha, J. Baugh, T. F. Havel, and D. G. Cory, “Selective coherence transfers in homonuclear dipolar coupled spin systems,” *Phys. Rev. A*, vol. 71, p. 020303, 2005.
- [22] C. Altafini, “Feedback control of spin systems,” *Quantum Information Processing*, in press, 2006.